Chapter 1

Microdynamics of Phononic Materials

Mahmoud I. Hussein,[a] Michael J. Frazier,[a] and Mohammad H. Abedinnasab[b]

[a] *Department of Aerospace Engineering Sciences, University of Colorado Boulder, Boulder, CO 80309-0429, USA*
[b] *Department of Mechanical Engineering, Sharif University of Technology, Tehran, 11365-9567, Iran*
mih@colorado.edu

1.1 Introduction

The fields of micromechanics and nanomechanics are concerned with the fine-scale mechanical behavior of materials. A micro- or nanoscale point of view allows for a more refined treatment of the material constituent behavior compared with traditional macroscale approaches. In this chapter, we will focus on a special type of materials, referred to as *phononic materials*, whereby the *microdynamical* behavior (or similarly, the *nanodynamical* behavior) can be tailored with remarkable precision. In doing so, we are able to alter the constitutive material behavior not only under static loading conditions as in other branches of micro- (and nano-) mechanics but also under low- and high-frequency dynamic loading conditions. This direct exposure, and access, to the inherent

Handbook of Micromechanics and Nanomechanics
Edited by Shaofan Li and Xin-Lin Gao

ISBN 978-981-4411-23-3 (Hardcover), 978-981-4411-24-0 (eBook)
www.panstanford.com

dynamical properties of materials has vigorously chartered a new direction in the entire field of mechanics, at a multitude of scales, and has already begun to impact numerous applications ranging from vibration control [1, 2], through subwavelength sound focusing [3, 4] and cloaking [5, 6], to reducing the thermal conductivity of semiconductors [7, 8] (a discussion of applications and references is provided in Refs. [9] and [10], and a recent special journal issue on the topic assembles some of the latest advances in the field [11].)

In this chapter, we present the basic theory of wave propagation in phononic materials focusing, for ease of exposition, on one-dimensional (1D) layered rod models. First we provide a background on the topic followed by an overview of the transfer matrix method, in conjunction with *Bloch's theorem*, for the exact analytical treatment of simple 1D phononic materials. In Section 1.2, we limit our attention to linear, conservative elastic media and an analysis based on the assumption of infinitesimal deformation. We then provide a detailed treatment of damping (Section 1.3) and geometric nonlinearity, i.e., finite deformation (Section 1.4). For each case, we start by examining the wave propagation characteristics in a homogenous medium (which is later used to represent the motion characteristics in a single layer of a periodically layered 1D phononic material), and then we extend our analysis to the overall 1D phononic material. As in the undamped problem, the treatment we present for the inclusion of damping is based on an exact analytical derivation. For the more complex nonlinear problem, however, we present a linearized approximate solution. Upon completing the derivations for each of the damped and nonlinear cases, we investigate the effects of damping and nonlinearity on the wave motion characteristics as a function of, respectively, damping intensity and amplitude of motion.

1.2 Wave Propagation in 1D Phononic Materials

1.2.1 *Background*

Phononic materials are elastic materials with prescribed phonon wave propagation properties. While the term "phonon" is formally

used in the physical sciences to describe vibration states in condensed matter at the atomic scale, in the present context, we use it to broadly describe elastic wave propagation modes. Like other types of materials, a phononic material has local intrinsic properties and is therefore mathematically treated as a medium that is spatially extended to infinity. At the most basic level, such a medium can be homogeneous and geometrically uniform. However, in order to realize rich and unique dynamical properties, some form of non-homogeneity and/or non-uniformity is needed and may be introduced in an ordered or disordered manner. In this chapter, we will focus on the former case, where phononic materials are constructed from a repeated array of identical *unit cells*.

There are two types of phononic materials of interest to us: *phononic crystals* and *periodic acoustic metamaterials*. Phononic crystals [1, 2, 3, 7, 8, 11, 12, 13] utilize elastic wave scattering at the unit cell interfaces to enable a mechanism of Bragg scattering where coherent interferences shape the overall wave propagation characteristics. Periodic acoustic (or elastic) metamaterials [4–6, 14], on the other hand, exhibit local resonances that directly alter the overall wave propagation characteristics from the baseline behavior pertaining to periodicity (a phenomenon often referred to as hybridization).

Bloch's theorem [15] provides the underlying mathematical framework for obtaining the fundamental wave propagation characteristics in phononic materials. Through this theorem, it is possible to obtain a relationship between frequency and wavenumber (or wave vector) whose graphical representation is referred to as the frequency band structure. An important feature of the frequency band structure in phononic materials, regardless of type, is the possibility of the existence of *band gaps*. A band gap is a frequency range in which no wave propagation is effectively permitted (see for example Refs. 16 and 17 for a discussion on the nature of band-gap opening mechanisms). In engineering applications, both band gaps and bands (frequency ranges where wave propagation is permitted) are widely utilized (see for example Refs. 18 and 19 on the utilization of band features for sound collimation and phase control, respectively). In a phononic crystal, a band gap can open only at frequencies corresponding to wavelengths on the order

of the size of the unit cell. In periodic acoustic metamaterials, however, a band gap may appear at lower frequencies, i.e., in the sub-wavelength regime. This is particularly useful as it significantly eases design restrictions on unit cell size. With careful size scaling and choice of the constituent material phases and their relative spatial distribution within the periodic unit cell, phononic materials can be designed and optimized for maximum band-gap width to midgap frequency ratio [20, 21] or for target dispersion band characteristics.

1.2.2 *Transfer Matrix Method*

We begin our dynamic analysis of a phononic material with the statement of the equation of motion. As mentioned earlier, we restrict ourselves to a 1D model, e.g., a rod, for which the equation of motion is

$$\sigma_{,x} + f = \rho u_{,tt}\,, \tag{1.1}$$

where $\sigma = \sigma(x,t)$, $f = f(x,t)$, $\rho = \rho(x)$, and $u = u(x,t)$ denote the stress, external body force (per unit length), material density, and displacement, respectively. As indicated, the value of each of these quantities is dependent upon the position x within the 1D medium and, with the exception of the material density, time t. Differentiation with respect to position and/or time is denoted by the appropriate subscript following a quantity. For example, $(\cdot)_{,x}$ indicates differentiation with respect to position while $(\cdot)_{,tt}$ signifies double differentiation with respect to time. In Eq. (1.1), we set $f = 0$ (external body forces are absent for free wave motion) and assume a linearly elastic material for which

$$\sigma = E u_{,x}\,, \tag{1.2}$$

where $E = E(x)$ is the material Young's modulus. Using Eq. (1.2), Eq. (1.1) in the absence of body forces becomes

$$E u_{,xx} = \rho u_{,tt}\,. \tag{1.3}$$

We may use Eq. (1.3) to study the propagation of waves in various 1D media. In particular, if we have a homogeneous, linearly elastic 1D rod of infinite extent (having no boundaries at which waves may reflect), then we may apply a plane wave solution of the form

$$u(x,t) = A\mathrm{e}^{\mathrm{i}(\kappa x - \omega t)}, \tag{1.4}$$

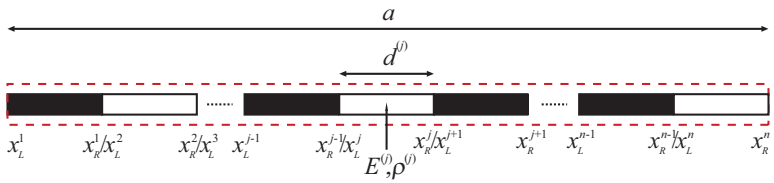

Figure 1.1 Continuous model of a two-phased 1D phononic crystal (periodic rod).

where A is the wave amplitude, κ is the wavenumber, ω is the temporal frequency of the traveling wave, and $\mathrm{i} = \sqrt{-1}$. Substituting Eq. (1.4) into Eq. (1.3) provides the linear dispersion relation

$$E\kappa^2 = \rho\omega^2. \tag{1.5}$$

This approach may also be applied to heterogeneous media provided the heterogeneity is periodic. In this case, we refer to Eq. (1.4) as Bloch's theorem, and it suffices to analyze only a single unit cell representing the unique segment that is repeated to generate the periodic medium and to apply periodic boundary conditions to this portion. In Fig. 1.1, we present a simple bi-material model of a 1D phononic crystal in the form of a layered periodic rod (where the unit cell is enclosed in a red dashed box). We denote the spatial lattice spacing of the 1D phononic crystal by the constant a. In order to analyze wave propagation in this periodic rod, we may choose from several techniques, including the finite difference, finite element, and transfer matrix methods. However, of these techniques, only the transfer matrix method offers an exact solution; the finite difference and finite element methods provide numerical approximations. Due to this advantage, we choose in this chapter to study the dynamical characteristics of 1D phononic crystals using the transfer matrix method, which we describe below (for more details, see Hussein *et al.* [21]). We note that our analysis can also be applied to a periodic acoustic metamaterial.

For a periodic medium composed of two or more material layers, the transfer matrix method uses the continuity conditions that exist between layers to relate displacement and stress values from one layer to the next. If the displacement and stress states at the boundary of one layer are known, then the corresponding states at the

opposite boundary (shared by the current and subsequent layers) can be derived from a simple matrix operation. The product of the repeated application of matrix operations for each layer across a unit cell yields a system matrix that relates the states at opposite ends of the entire unit cell. This system matrix is then utilized in conjunction with Bloch's theorem to obtain an eigenvalue problem whose solution generates the dispersion curves of the 1D phononic crystal. The mathematical derivation of this method is provided below.

For an arbitrary homogeneous layer j in the unit cell, the associated material properties, which are constant, are denoted as $E^{(j)}$ and $\rho^{(j)}$. The longitudinal velocity in layer j is therefore $c^{(j)} = \sqrt{E^{(j)}/\rho^{(j)}}$. The layer is bordered by layer $j-1$ on the left and layer $j+1$ on the right. Given the thickness of an arbitrary layer of the unit cell is $d^{(j)}$, the cell length is $a = \sum_{j=1}^{n} d^{(j)}$ for a unit cell with n layers. Following this notation, the solution to Eq. (1.3) is formed from the superposition of forward (transmitted) and backward (reflected) traveling waves with a harmonic time dependence,

$$u(x,t) = [A_+^{(j)} \mathrm{e}^{\mathrm{i}\kappa^{(j)}x} + A_-^{(j)} \mathrm{e}^{-\mathrm{i}\kappa^{(j)}x}]\mathrm{e}^{-\mathrm{i}\omega t}, \tag{1.6}$$

where $\kappa^{(j)} = \omega/c^{(j)}$ is the layer wavenumber. We can write the spatial components of Eqs. (1.2) and (1.6) in compact form as

$$\begin{bmatrix} u(x) \\ \sigma(x) \end{bmatrix} = \begin{bmatrix} 1 & 1 \\ \mathrm{i}Z^{(j)} & -\mathrm{i}Z^{(j)} \end{bmatrix} \begin{bmatrix} A_+^{(j)} \mathrm{e}^{\mathrm{i}\kappa^{(j)}x} \\ A_-^{(j)} \mathrm{e}^{-\mathrm{i}\kappa^{(j)}x} \end{bmatrix} = \mathbf{B}_j \begin{bmatrix} A_+^{(j)} \mathrm{e}^{\mathrm{i}\kappa^{(j)}x} \\ A_-^{(j)} \mathrm{e}^{-\mathrm{i}\kappa^{(j)}x} \end{bmatrix}, \tag{1.7}$$

where $Z^{(j)} = E^{(j)}\kappa^{(j)}$. As mentioned earlier, there are two conditions that must be satisfied at the layer interfaces: (1) the continuity of displacement and (2) the continuity of stress. This allows us to substitute the relation $x_R^{(j)} = x_L^{(j)} + d^{(j)}$ (where $x_R^{(j)}$ and $x_L^{(j)}$ denote the position of the right and left boundary, respectively, of layer j) into Eq. (1.7) and thus relate the displacement and stress at $x_L^{(j)}$ to those at $x_R^{(j)}$,

$$\begin{aligned} \begin{bmatrix} u\left(x_R^{(j)}\right) \\ \sigma\left(x_R^{(j)}\right) \end{bmatrix} &= \mathbf{B}_j \begin{bmatrix} \mathrm{e}^{\mathrm{i}\kappa^{(j)}d^{(j)}} & 0 \\ 0 & \mathrm{e}^{-\mathrm{i}\kappa^{(j)}d^{(j)}} \end{bmatrix} \begin{bmatrix} A_+^{(j)} \mathrm{e}^{\mathrm{i}\kappa^{(j)}x_L^{(j)}} \\ A_-^{(j)} \mathrm{e}^{-\mathrm{i}\kappa^{(j)}x_L^{(j)}} \end{bmatrix} \\ &= \mathbf{B}_j \mathbf{D}_j \begin{bmatrix} A_+^{(j)} \mathrm{e}^{\mathrm{i}\kappa^{(j)}x_L^{(j)}} \\ A_-^{(j)} \mathrm{e}^{-\mathrm{i}\kappa^{(j)}x_L^{(j)}} \end{bmatrix}. \end{aligned} \tag{1.8}$$

By setting $x = x_L^{(j)}$ in Eq. (1.7), we may rewrite Eq. (1.8) as

$$\begin{bmatrix} u\left(x_R^{(j)}\right) \\ \sigma\left(x_R^{(j)}\right) \end{bmatrix} = \mathbf{B}_j \mathbf{D}_j \mathbf{B}_j^{-1} \begin{bmatrix} u\left(x_L^{(j)}\right) \\ \sigma\left(x_L^{(j)}\right) \end{bmatrix} = \mathbf{T}_j \begin{bmatrix} u\left(x_L^{(j)}\right) \\ \sigma\left(x_L^{(j)}\right) \end{bmatrix}, \tag{1.9}$$

where $\mathbf{T}_j$, the *transfer matrix* for layer j, has the expanded form

$$\mathbf{T}_j = \begin{bmatrix} \cos(\kappa^{(j)} d^{(j)}) & (1/Z^{(j)}) \sin(\kappa^{(j)} d^{(j)}) \\ -Z^{(j)} \sin(\kappa^{(j)} d^{(j)}) & \cos(\kappa^{(j)} d^{(j)}) \end{bmatrix}. \tag{1.10}$$

As previously stated, Eq. (1.9) relates the displacement and stress at $x_L^{(j)}$ to those at $x_R^{(j)}$ of the same layer j. However, since the construction of the transfer matrix is valid for any layer and $x_L^{(j)} \equiv x_R^{(j-1)}$, the result in Eq. (1.9) can be extended recursively across several layers. In the interest of brevity, let $\mathbf{y}(\cdot) = [u(\cdot)\, \sigma(\cdot)]^{\mathrm{T}}$, thus,

$$\begin{aligned} \mathbf{y}(x_R^1) &= \mathbf{T}_1 \mathbf{y}(x_L^1) = \mathbf{y}(x_L^2), \\ \mathbf{y}(x_R^2) &= \mathbf{T}_2 \mathbf{y}(x_L^2) = \mathbf{T}_2 \mathbf{T}_1 \mathbf{y}(x_L^1) = \mathbf{y}(x_L^3), \\ \mathbf{y}(x_R^3) &= \mathbf{T}_3 \mathbf{y}(x_L^3) = \mathbf{T}_3 \mathbf{T}_2 \mathbf{T}_1 \mathbf{y}(x_L^1) = \mathbf{y}(x_L^4), \\ &\vdots \\ \mathbf{y}(x_R^n) &= \mathbf{T}_n \mathbf{T}_{n-1} \cdots \mathbf{T}_1 \mathbf{y}(x_L^1) = \mathbf{T}\mathbf{y}(x_L^1). \end{aligned} \tag{1.11}$$

Ultimately, the displacement and stress at the left end of the first layer ($x = x_L^1$) in a unit cell are related to those at the right boundary of the *nth* layer ($x = x_R^n$) by the *cumulative transfer matrix*, $\mathbf{T}$.

Now we turn to Bloch's theorem, which states that the time-harmonic response at a given point in a unit cell is the same as that of the corresponding point in an adjacent unit cell except for a phase difference of $\mathrm{e}^{\mathrm{i}\kappa a}$, where κ is the wavenumber corresponding to the overall wave propagation across the periodic 1D phononic crystal. This relation is given by $f(x + a) = \mathrm{e}^{\mathrm{i}\kappa a} f(x)$, which when applied to the states of displacement and stress across a unit cell gives

$$\boldsymbol{y}(x_R^n) = \mathrm{e}^{\mathrm{i}\kappa a} \boldsymbol{y}(x_L^1). \tag{1.12}$$

Combining Eqs. (1.11) and (1.12) yields the eigenvalue problem

$$[\mathbf{T} - \mathbf{I}\gamma]\mathbf{y}(x_L^1) = \mathbf{0}, \tag{1.13}$$

where $\gamma = \mathrm{e}^{\mathrm{i}\kappa a}$. The solution of Eq. (1.13), which appears in complex-conjugate pairs, provides the dispersion relations $\kappa(\omega)$ for the 1D

phononic crystal. Real-valued wavenumbers, calculated from γ using Eq. (1.14), support propagating wave modes, whereas imaginary wavenumbers, extracted from γ using Eq. (1.15), represent those modes which decay in space:

$$\kappa_R = \frac{1}{a}\mathrm{Re}\left[\frac{1}{\mathrm{i}}\ln\gamma\right], \tag{1.14}$$

$$\kappa_I = \frac{1}{a}\mathrm{Im}\left[\frac{1}{\mathrm{i}}\ln\gamma\right]. \tag{1.15}$$

1.3 Treatment of Damping

Damping is an innate property of materials and structures. Its consideration in the study of wave propagation is important because of its association with energy dissipation. We can concisely classify the sources of damping in phononic materials into three categories, depending on the type and configuration of the unit cell. These are: (1) bulk material-level dissipation stemming from deformation processes (e.g., dissipation due to friction between internal crystal planes that slip past each other during deformation); (2) dissipation arising from the presence of interfaces or joints between different components (e.g., lattice structures consisting of interconnected beam elements [1, 23]); and (3) dissipation associated with the presence of a fluid within the periodic structure or in contact with it. In general, the mechanical deformations that take place at the bulk material level, or similarly at interfaces or joints, involve microscopic processes that are not thermodynamically reversible [24]. These processes account for the dissipation of the oscillation energy in a manner that fundamentally alters the macroscopic dynamical characteristics including the shape of the frequency band structure. Similar yet qualitatively different effects occur due to viscous dissipation in the presence of a fluid. While the representation of the inertia and elastic properties of a vibrating structure is adequately accounted for, finding an appropriate damping model to describe observed experimental behavior can be a daunting task. This is primarily due to the difficulty in identifying the state variables upon which the damping forces depend and in formulating the best

functional representation once a set of state variables is determined [25]. A review of established approaches for the treatment of damping in linear systems is available in Refs. [25] and [26]. As for wave propagation in damped phononic materials, the reader is referred to Refs. [27] and [28] and references therein.

1.3.1 *Viscously Damped Waves in 1D Homogeneous Media*

In Section 1.2.2, we introduced the transfer matrix method as a means to analyze wave propagation in the disparate layers of a 1D phononic crystal. These layers were assumed to be linearly elastic and conservative, that is, no energy is lost as waves propagate within the layers and through the layer interfaces. On this basis, the relation $\kappa^{(j)} = \omega/c^{(j)}$ holds in layer j. However, in actual material systems, energy is dissipated by a variety of mechanisms as stated above. It is therefore useful to consider the effects of energy dissipation (damping) in the underlying transfer matrix formulation.

Due to the diversity and complexity of dissipative mechanisms, the development of a universal damping model stands as a major challenge. A rather simple model proposed by Rayleigh [29], one which we will consider, is the *viscous damping* model in which the instantaneous generalized velocity, $u_{,t}$, is the only relevant state variable in the determination of the damping force f_d [26]. The consequences for a homogeneous 1D medium, e.g., a rod, is that the stress is not only related to the strain, $u_{,x}$, following Hooke's law, but also a function of the strain rate, $u_{,xt}$, involving a constant, η (which, in essence, represents the *viscosity*). The constitutive relationship then becomes

$$\sigma = E u_{,x} + \eta u_{,xt} \,. \tag{1.16}$$

Substitution of Eq. (1.16) into Eq. (1.1) (recall $f = 0$) yields the general equation for wave propagation in a viscously damped homogeneous rod,

$$E u_{,xx} + \eta u_{,xxt} = \rho u_{,tt} \,. \tag{1.17}$$

This naturally leads to a different relationship between κ and ω than was stated in Eq. (1.5). To see this, we generalize the temporal component of Eq. (1.4) to $e^{\lambda t}$ to allow for dissipation in time in

addition to space [27, 28, 30, 31], that is,

$$u(x,t) = A\mathrm{e}^{\mathrm{i}\kappa x+\lambda t}. \tag{1.18}$$

Substituting Eq. (1.18) into Eq. (1.17) yields the characteristic equation

$$-E\kappa^2 - \lambda\eta\kappa^2 = \lambda^2\rho, \tag{1.19}$$

which, following Cady [30], has the solutions

$$\lambda = -\frac{\eta\kappa^2}{2\rho} \pm \mathrm{i}\kappa\sqrt{\frac{E}{\rho} - \left(\frac{\eta\kappa}{2\rho}\right)^2}. \tag{1.20}$$

The association of Eq. (1.5) with Eq. (1.20) is easily verified in the absence of dissipation ($\eta = 0$) where $\lambda = -\mathrm{i}\omega$. In the presence of dissipation, however, λ is complex and reflects the form suggested by Hussein [27] and Hussein and Frazier [28]

$$\lambda = -\xi\omega \pm \mathrm{i}\omega_\mathrm{d}, \tag{1.21}$$

where ω_d and ξ are the wavenumber-dependent damped wave frequency and associated damping ratio, respectively.

At present, the value of the viscosity η is undefined. In principle, any value guaranteeing a positive rate of dissipation is acceptable. For our treatment of viscously damped homogeneous media, we will adopt a model considered by Rayleigh [29], and define the viscosity to be proportional to the elasticity, $\eta = qE$, where q is a constant of proportionality. Thus, Eq. (1.20) becomes

$$\begin{aligned}\lambda &= -\frac{qE\kappa^2}{2\rho} \pm \mathrm{i}\kappa\sqrt{\frac{E}{\rho} - \left(\frac{qE\kappa}{2\rho}\right)^2} \\ &= -\left(\frac{qc\kappa}{2}\right)c\kappa \pm \mathrm{i}c\kappa\sqrt{1 - \left(\frac{qc\kappa}{2}\right)^2},\end{aligned} \tag{1.22}$$

where $c = \sqrt{E/\rho}$. Using Eq. (1.21) and with the previously stated relation $\omega = c\kappa$, the damped wave frequency and damping ratio may be extracted from Eq. (1.22) as

$$\omega_\mathrm{d}(\kappa; q) = c\kappa\sqrt{1 - \left(\frac{qc\kappa}{2}\right)^2} \tag{1.23}$$

and

$$\xi = \frac{qc\kappa}{2}. \tag{1.24}$$

In this section, we considered a homogeneous medium (a rod) in which κ is the global wavenumber. In the following section, in

which we consider a heterogeneous, periodically layered rod – a 1D phononic crystal – we will see the return of the layer wavenumber, $\kappa^{(j)}$.

1.3.2 *Viscously Damped Waves in 1D Phononic Materials*

As presented, the transfer matrix method is prepared for either the absence or presence of dissipation; the distinction is made in the definition of $Z^{(j)}$ and $\kappa^{(j)}$. In general, $Z^{(j)} = \kappa^{(j)}(E^{(j)} + \eta^{(j)}\lambda)$; however, specific to our earlier prescription for η, $Z^{(j)} = \kappa^{(j)}E^{(j)}(1 + q\lambda)$. Note that this form collapses to the earlier definition of $Z^{(j)}$ for the undamped case where η (or q) is set equal to zero. In the condition of undamped wave propagation, the relationship between the wavenumber and the frequency has already been presented: $\kappa^{(j)} = \omega/c^{(j)}$. A similar relationship between the wavenumber and the damped wave frequency for layer j can be developed from Eq. (1.23). Given the quadratic form of Eq. (1.23),

$$\frac{q^2[c^{(j)}]^4}{4}[\kappa^{(j)}]^4 - [c^{(j)}]^2[\kappa^{(j)}]^2 + \omega_{\mathrm{d}}^2 = 0, \tag{1.25}$$

we can formulate two complex-conjugate solutions for $[\kappa^{(j)}]^2$, from which we develop the explicit relation

$$\kappa^{(j)} = \pm\frac{1}{qc^{(j)}}\sqrt{2\left(1 \pm \sqrt{1 - q^2\omega_{\mathrm{d}}^2}\right)}. \tag{1.26}$$

Given the placement of q in the denominator of Eq. (1.26), it is apparent that the equation is only valid if q has a nonzero value. Alternatively, q can be set to the zero value (or any positive value) in Eq. (1.25) without difficulty, and then $\kappa^{(j)} = \omega_{\mathrm{d}}/c^{(j)}$ ($\omega_{\mathrm{d}} \equiv \omega$ in an undamped system) is readily recovered.

Now we will use Eq. (1.26) and the transfer matrix method to obtain the dispersion curves of a viscously damped 1D phononic crystal, in particular, the periodic bi-material rod in Fig. 1.1 (a similar analysis can be applied to a periodic acoustic metamaterial). We consider a unit cell with $n = 2$ and $d^{(1)} = d^{(2)}$. A specific set of material parameters listed in Table 1.1 provide a reference for our exposition; these two material phases comprise our example phononic crystal. We offer a suite of numerical case studies to illustrate the effects of dissipation. In each case, the damping

Table 1.1 Phononic crystal properties

ABS polymer	$\rho^{(1)} = 1040\ \text{kg/m}^3$	$E^{(1)} = 2.4\text{GPa}$
Aluminum	$\rho^{(2)} = 2700\ \text{kg/m}^3$	$E^{(2)} = 68.9\text{GPa}$

intensity q is varied to give a good representation of the dissipative effects. In Fig. 1.2, we show the frequency (non-dimensional) and damping ratio band structures for this model. Each plot is divided into positive and negative wavenumber (non-dimensional) domains representing the propagating and evanescent waves, respectively. The evanescent wavenumbers are not negative; rather, they are indicated as such to emphasize their attenuating nature (which arises from the multiplication of the imaginary part of the wavenumber with a unit imaginary number).

We observe in Fig. 1.2 that as the damping intensity q increases, the optical branches drop rapidly while the acoustic branch experiences relatively little change – the result is a reduction in the size of the band gap. This behavior is readily explained by the corresponding band structure of the damping ratio diagram. Higher branches in the diagram indicate a greater damping ratio and so the rate at which a mode descends is correlated to its position. The damping ratio curves evolve in a synchronous manner with the dissipation intensity; ascending the band diagram accordingly. As q increases, higher branches in the damping ratio band diagram meet/exceed unity in part or in entirety (not shown). In these instances, similar to structural dynamics of finite systems, we assert that these branches are critically damped or over-damped and that no propagation is permitted (i.e., the frequency band has collapsed to zero). It should be noted that for identical levels of prescribed damping, the band diagrams would appear radically different if the temporal component of the solution $u(x, t)$ had been prescribed as $\mathrm{e}^{-\mathrm{i}\omega t}$ rather than $\mathrm{e}^{\lambda t}$. In fact, with the assumption $\lambda = -\mathrm{i}\omega$, the damping ratio band diagram would not be defined. As such, Eq. (1.18) in the context of periodic media may be referred to as the *generalized Bloch's theorem*. Employment of this form allows us to obtain the dispersion relation for damped free wave propagation. Should we have adopted the standard form of the theorem, in which the frequencies are assumed to be real, we would have obtained a solution for the propagation of damped waves with prescribed frequencies.

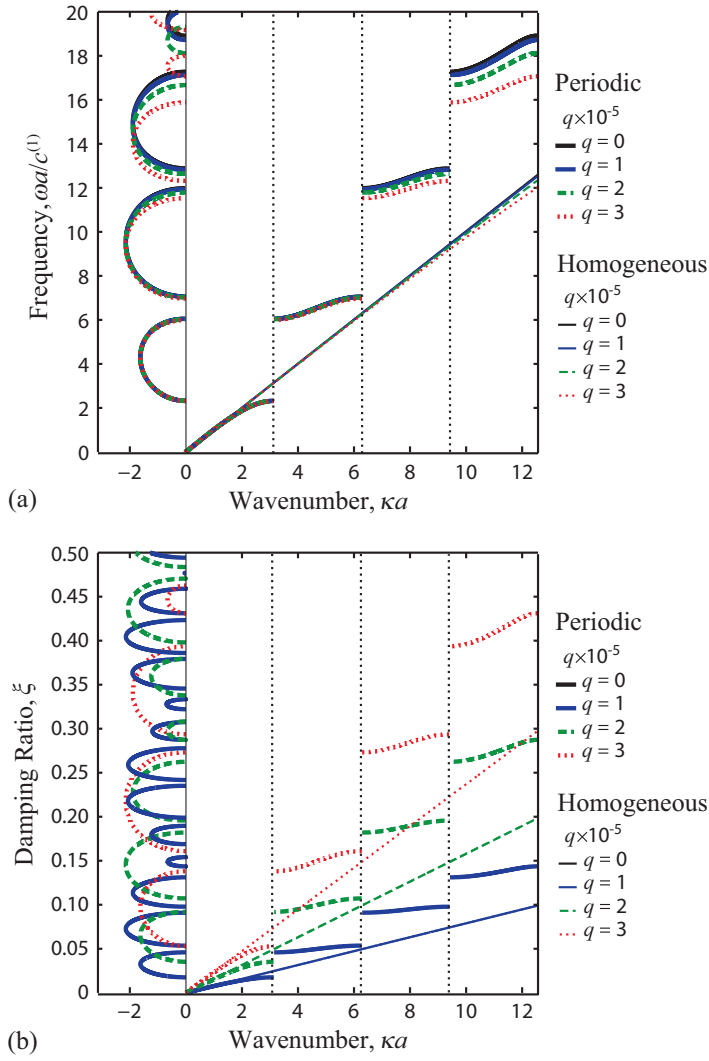

Figure 1.2 Frequency (a) and damping ratio (b) band structure for a viscously damped 1D phononic crystal consisting of two layers in the unit cell. For comparison, the dispersion curves for the undamped problem are included. Also, corresponding dispersion curves for a statically equivalent homogenous rod are overlaid.

1.4 Treatment of Nonlinearity

The majority of investigations of wave motion in elastic solids are based on linear analysis, that is, linear constitutive laws and linear strain–displacement relationships are assumed (see Refs. 32 and 33, and references therein). The incorporation of nonlinear effects has nevertheless been considered and is receiving increasing attention because, as in damping, it allows for a more accurate description of the underlying motion and facilitates the study of complex dynamical phenomena [34–41]. Also similar to damping, the effects of nonlinearity on the dispersion of waves in waveguides could be utilized to enrich the design of materials and structural components in numerous engineering applications. Current applications for nonlinear elastic wave propagation studies include nonlinear vibration analysis [42], dislocation and crack dynamics analysis [43, 44], geophysical and seismic motion analysis [45], material characterization and nondestructive evaluation [46, 47] and biomedical imaging [48].

Finite amplitude wave propagation in elastic solids is a subset among the broader class of nonlinear wave propagation problems. From a mathematical perspective, a formal treatment of finite deformation requires the incorporation of an exact nonlinear strain tensor in setting up the governing equations of motion. As a result, the emerging analysis permits large and finite strain fields as opposed to small and infinitesimal strain fields. A large portion of research on finite amplitude waves considers initially strained materials (see, for example, the early studies by Truesdell [34] and Green [35], and Ogden [39] for an extensive discussion on the topic). Furthermore, analysis of finite-amplitude waves in solids often involve small parameters or asymptotic expansions (see Norris [40] for a review). Among the relatively recent works that focused on finite-amplitude plane waves in materials subjected to a large static finite deformation include those of Boulanger and Hayes [49], Boulanger *et al.* [50] and Destrade and Saccomandi [51]. Focusing on rods, modeled in one dimension or higher, many studies considered small but finite amplitude waves for both incompressible and compressible materials (e.g., [52–56]). Of particular relevance is a recent study by Zhang and Liu [57] in

which an exact equation of motion for a rod and an approximate equation of motion for an Euler-Bernoulli beam were derived under the condition of finite deformation. In all these studies, and others in the literature concerned with finite-strain wave motion in homogeneous media, generally the interest has been in obtaining spatial/temporal solutions, or solutions at certain physical limits, rather than complete dispersion relations. In the context of nonlinear phononic materials, there are several studies that follow the premise of Bloch analysis. These include investigations utilizing the method of multiple scales [58, 59], perturbation analysis [60, 61] and the harmonic balance method [62, 63]. In Ref. [64], nonlinear wave phenomena in periodic granular chains were examined by experiments.

In this section, we provide a theoretical treatment of finite-strain dispersion; first we present an exact analysis for a 1D homogenous medium (e.g., a homogeneous rod), and we follow with an approximate analysis of a 1D phononic crystal (e.g., a periodic rod). In both problems, our approach is not limited by the amplitude of the traveling wave. Starting with Hamilton's principle, we consider axial deformation to represent longitudinal motion. We derive the equation of motion and the implicit dispersion relation from which we obtain the explicit frequency versus wavenumber solution for each of the homogeneous and periodic cases.

1.4.1 *Finite-Strain Waves in 1D Homogenous Media*

In this section, we derive the equation of motion and the dispersion relation for elastic wave motion in a homogeneous rod (assuming slender cross section) as an example of a 1D homogeneous medium. In our derivation, all terms in the nonlinear strain tensor are retained and no high order terms emerging from the differentiations are subsequently neglected. To verify our theoretical approach, we examine wave propagation in a corresponding finite rod by means of a standard finite-strain numerical simulation (using finite element analysis) and compare the response with our derived dispersion relation. The formulations we develop allow us to examine the effect of finite deformation on the frequency dispersion curves in rods, or in the context of 1D plane wave motion in a bulk medium without

consideration of lateral effects. Further details on nonlinear analysis of homogeneous media are available in Ref. [65].

1.4.1.1 Equation of motion

Introducing Δ as the elastic displacement, the exact complete Green–Lagrange strain field in a rod is given by

$$\epsilon = \frac{\partial \Delta}{\partial s} + \frac{1}{2}\left(\frac{\partial \Delta}{\partial s}\right)^2, \tag{1.27}$$

where the first and second terms on the RHS represent the linear and nonlinear parts, respectively, and s is the Lagrangian longitudinal coordinate. The elastic displacement field for the rod, Δ, is equal to axial displacement, u,

$$\Delta = u. \tag{1.28}$$

Using Hamilton's principle, we write the equation of motion for a rod under uniaxial stress as

$$\int_0^t (\delta T - \delta U^e + \delta W^{nc})\mathrm{d}t = 0, \tag{1.29}$$

where T, U^e, and W^{nc} denote kinetic energy, elastic potential energy and the work done by external nonconservative forces and moments, respectively, and t denotes time. Neglecting the effects of lateral inertia and using integration by parts, the variation of elastic potential energy is

$$\delta U^e = \int_0^l \int_A (\sigma \delta \epsilon)\mathrm{d}A\ \mathrm{d}s, \tag{1.30}$$

where σ and ϵ are the axial stress and axial strain, respectively, and l denotes the length of a portion of the rod. We chose to base our analysis on the Cauchy stress. The stress–strain relationship is modeled following Hooke's law,

$$\sigma = E\epsilon, \tag{1.31}$$

where E is the Young's modulus. Using Eq. (1.30), and with the aid of integration by parts, we can now write the variation of elastic potential energy as

$$\delta U^e = \int_0^l \left\{\frac{1}{2} E A h(h^2 - 1)\delta u'\right\} \mathrm{d}s, \tag{1.32}$$

where $u' = du/ds = u_{,s}$ and h is an agent variable defined as

$$h = 1 + u'. \tag{1.33}$$

The variation of non-conservative forces and moments is given in terms of the variation of axial deformation, u, and the distributed external axial load q_u,

$$\delta W^{nc} = \int_0^l (q_u \delta u) \mathrm{d}s. \tag{1.34}$$

The variation of kinetic energy is also obtained using integration by parts and is given as

$$\delta T = -\rho A \int_0^l (u_{,tt}\, \delta u) \mathrm{d}s. \tag{1.35}$$

Substitution of Eqs. (1.32), (1.34), and (1.35) into Eq. (1.29) produces the equation of motion and the companion boundary conditions given in Eqs. (1.36) and (1.37), respectively:

$$\int_0^t \left\{ \int_0^l (A_1 \delta u) ds + (B_1 \delta u + \overline{B}_1 \delta u')\big|_{s=0}^{s=l} \right\} \mathrm{d}t = 0, \tag{1.36}$$

$$(B_1 = 0 \text{ or } u = 0) \text{ and } (\overline{B}_1 = 0 \text{ or } u' = 0). \tag{1.37}$$

We can now write an exact nonlinear equation of motion of a 1D rod under finite deformation as

$$A_1 = 0: \quad \rho A u_{,tt} = \frac{1}{2} E A (3h^2 - 1) u'' + q_u. \tag{1.38}$$

The section load, namely the axial force, is

$$B_1 = \frac{1}{2} E A h (h^2 - 1) \tag{1.39a}$$

$$\overline{B}_1 = 0. \tag{1.39b}$$

If the axial deformation is infinitesimal, then u' is small and from Eq. (1.33), $h \approx 1$. Substitution of $h = 1$ into Eq. (1.38) leads to

$$A_1 = 0: \quad \rho A u_{,tt} = E A u'' + q_u, \tag{1.40}$$

which is the equation of motion describing infinitesimal axial deformation.

1.4.1.2 Dispersion relation

Using Eq. (1.33), we rewrite Eq. (1.38) as

$$u_{,tt} - c^2 u'' = \frac{1}{2}[3c^2(u')^2 + c^2(u')^3]', \tag{1.41}$$

Equation (1.41) is integrable despite it being nonlinear. Differentiating Eq. (1.41) once with respect to s gives

$$(u_{,tt})' - c^2 u^{(3)} = \frac{1}{2}[3c^2(u')^2 + c^2(u')^3]''. \tag{1.42}$$

Defining $\overline{u} = u'$ and $\tau = \omega_{\text{fin}}\text{t}$, where ω_{fin} is the frequency of a traveling wave, Eq. (1.42) becomes

$$\omega_{\text{fin}}^2 \overline{u}_{,\tau\tau} - c^2 \overline{u}'' = \frac{1}{2}[3c^2(\overline{u})^2 + c^2(\overline{u})^3]''. \tag{1.43}$$

Defining $z = |\kappa|s + \tau$, where κ is the wavenumber of a harmonic wave, we rewrite Eq. (1.43) as

$$\omega_{\text{fin}}^2 \overline{u}_{,zz} - c^2\kappa^2 \overline{u}_{,zz} = \frac{1}{2}\kappa^2[3c^2(\overline{u})^2 + c^2(\overline{u})^3]_{,zz} \tag{1.44}$$

where now the explicit dependency on s and τ has been eliminated. Integrating Eq. (1.44) twice leads to

$$\omega_{\text{fin}}^2 \overline{u} - c^2\kappa^2 \overline{u} = \frac{1}{2}\kappa^2[3c^2(\overline{u})^2 + c^2(\overline{u})^3], \tag{1.45}$$

or

$$(\omega_{\text{fin}}^2 - c^2\kappa^2)\overline{u} - \frac{c^2\kappa^2}{2}[3\overline{u}^2 + \overline{u}^3] = 0. \tag{1.46}$$

We note that in our integration of Eq. (1.44) we get nonzero constants of integration in the form of polynomials in z. Since these represent secular terms we have set them all equal to zero in light of our interest in the dispersion relation. Selecting the positive root of Eq. (1.46) we get

$$\overline{u}(z) = \frac{-3 + \sqrt{1 + 8\omega_{\text{fin}}^2/c^2\kappa^2}}{2}. \tag{1.47}$$

Since $\overline{u} = u_{,s}$, we recognize that $\overline{u} = |\kappa|u_{,z}$ and therefore Eq. (1.47) represents a first-order nonlinear ordinary differential equation with z and u as the independent and dependent variables, respectively.

Now we return to Eq. (1.41) and consider for initial conditions a sinusoidal displacement field, with amplitude B and a zero phase in time, and a zero velocity field. Following the change of variables we have introduced, these initial conditions essentially correspond to the following restrictions on the $\overline{u}(z)$ function given in Eq. (1.47):

$$\overline{u}(0) = |\kappa| B, \quad \overline{u}_{,z}(0) = 0. \tag{1.48}$$

We note that since z describes a space-time wave phase, the restrictions given in Eq. (1.48) represent initial conditions on the wave phase. The importance of these initial conditions is that they incorporate the effect of the wave amplitude, B, into the finite deformation dispersion relation. Applying Eq. (1.48) to Eq. (1.47) allows us to use the latter to solve for ω_{fin} for a given value of κ at $z = 0$. Thus we obtain an exact dispersion relation for wave motion in a rod under finite deformation, which is

$$\omega_{\text{fin}}(\kappa; B) = \sqrt{\frac{2 + 3B|\kappa| + (B\kappa)^2}{2}}\omega, \tag{1.49}$$

where ω is the frequency based on infinitesimal deformation,

$$\omega(\kappa) = c|\kappa|. \tag{1.50}$$

By taking the limit, $\lim_{B\to 0} \omega_{\text{fin}}(\kappa; B)$, in Eq. (1.49) we recover Eq. (1.50) which is the standard linear dispersion relation for a rod, as shown by Billingham and King [66].

For demonstration, two amplitude-dependent finite deformation dispersion curves for an infinite rod based on Eq. (1.49) are plotted in Fig. 1.3. These dispersion curves provide an exact fundamental description of how an elastic harmonic wave locally, and instantaneously, disperses in an infinite rod under the dynamic condition of amplitude-dependent finite deformation. Superimposed in the same figure is the dispersion curve based on infinitesimal deformation, i.e., Eq. (1.50). We observe that the deviation between a finite deformation curve and the infinitesimal deformation curve increases with wavenumber, and the effect of the wave amplitude on this deviation appears to be steady (in the wavenumber range considered) as B is increased.

In addition, the results from standard finite element simulations of a finite version of the rod with length L are presented. A prescribed sinusoidal displacement with frequency $\hat{\omega}$ and amplitude

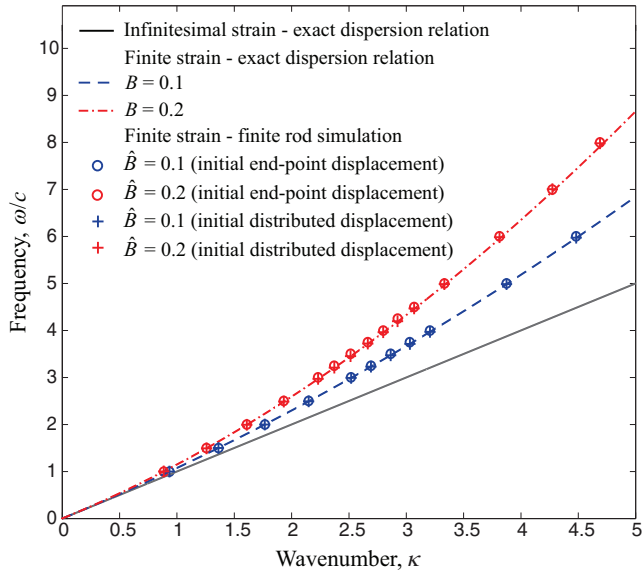

Figure 1.3 Frequency dispersion curves for a homogeneous rod [65]. The finite-strain dispersion relation is based on Eq. (1.49); the infinitesimal strain dispersion relation is based on Eq. (1.50).

$\hat{B}$, i.e., $u(L\,,t) = \hat{B}\sin(\hat{\omega}t)$, was applied to the tip of the rod with free-free boundary conditions. The finite-deformation finite element model consisted of 60 piecewise linear elements with equal lengths, and each node consisted of two degrees of freedom, u and u'. Equal time steps of 10^{-4} [s] were considered in the numerical integration, which was implemented using MATLAB's *ode*113 solver [67]. The wavenumber has been recorded by observing the wavelength after one period of temporal oscillation of the tip (i.e., excitation point) of the rod, and plotted as a function of frequency $\hat{\omega}$ for two given amplitudes. This recording is meaningful because the wave's harmonic form is effectively still maintained during the first oscillation cycle in the vicinity of the excitation point. The data points from this simulation (of a finite rod) match very well with the analytically derived exact dispersion curve (corresponding to an infinite rod). While the wave considered at the tip of the excited rod will evolve, under finite strain, into a complex form as

it propagates into the rod, this correlation provides a validation that a given harmonic wave will locally and instantaneously disperse in a manner exactly as described by Eq. (1.49). The other simulation data shown in the figure correspond to the response due to initial sinusoidal displacements at a prescribed wavenumber (applied when the rod is in a state of rest). Here we measure the frequency of the oscillations as the wave propagates within the first temporal cycle. The simulation parameters are the same to those in the initial end-point prescribed displacement runs. As illustrated in the figure, this simulation further validates the analytical dispersion relation given by Eq. (1.49).

1.4.2 *Finite-Strain Waves in 1D Phononic Materials*

The transfer matrix method presented in Section 1.2.2 can be used to obtain an approximate dispersion relation for a 1D phononic crystal under finite deformation. The approximation arises in the construction of the transfer matrix which is based on a linear strain-displacement relationship [see Eqs. (1.2) and (1.7)]. The application of the technique for this problem is similar to its application to the damped 1D phononic crystal problem presented in Section 1.3.2, with the only differences being the definition of the $Z^{(j)}$ function (for which we now use the undamped form) and the $\kappa^{(j)}(\omega_\propto)$ function (where $\propto = \mathrm{d}$ in the damping problem and $\propto = \mathrm{fin}$ in the finite deformation problem). For a 1D damped phononic material, the former function is given in Eq. (1.26). Now we seek a similar function for wave motion under finite deformation in layer j.

First we rewrite Eq. (1.49) explicitly for layer j,

$$\omega_{\mathrm{fin}} = c^{(j)}\kappa^{(j)}\sqrt{\frac{2 + 3B\kappa^{(j)} + [B\kappa^{(j)}]^2}{2}}, \tag{1.51}$$

which may be cast as the following 4th order characteristic equation:

$$[\kappa^{(j)}]^2(1 + B\kappa^{(j)})(2 + B\kappa^{(j)}) - 2\frac{\omega_{\mathrm{fin}}^2}{\left[c^{(j)}\right]^2} = 0. \tag{1.52}$$

Solving Eq. (1.52) gives

$$\kappa_{1,2}^{(j)} = \frac{1}{12B}\left(-9 + P^{(j)} \mp \sqrt{Q^{(j)} - R^{(j)}}\right), \tag{1.53a}$$

$$\kappa_{3,4}^{(j)} = -\frac{1}{12B}\left(9 + P^{(j)} \pm \sqrt{Q^{(j)} + R^{(j)}}\right), \tag{1.53b}$$

where

$$P^{(j)} = \sqrt{\frac{33c^{(j)}A^{(j)} + 12\left(-24B^2\omega_{\text{fin}}^2 + 4\left[c^{(j)}\right]^2 + \left[A^{(j)}\right]^2\right)^2}{c^{(j)}A^{(j)}}}, \tag{1.54a}$$

$$Q^{(j)} = \frac{66c^{(j)}A^{(j)} - 48\left(-6B^2\omega_{\text{fin}}^2 + \left[c^{(j)}\right]^2\right) - 12\left[A^{(j)}\right]^2}{c^{(j)}A^{(j)}}, \tag{1.54b}$$

$$R^{(j)} = \frac{54\sqrt{3}}{\sqrt{\frac{11c_0^{(j)}A^{(j)} + 4\left(-24B^2\omega_{\text{fin}}^2 + 4\left[c^{(j)}\right]^2 + \left[A^{(j)}\right]^2\right)}{c^{(j)}A^{(j)}}}} \tag{1.54c}$$

and

$$A^{(j)} = \left(-99B^2\omega_{\text{fin}}^2 c^{(j)} + 8\left[c^{(j)}\right]^3 + 3B\omega_{\text{fin}}\sqrt{\left(1536B^2 + 321\left[c^{(j)}\right]^2\right)B^2\omega_{\text{fin}}^4 - 48\left[c^{(j)}\right]^4}\right)^{1/3}. \tag{1.54d}$$

Now we will use Eq. (1.53) and the transfer matrix method to obtain an approximation of the finite strain dispersion curves of a 1D phononic crystal that has the same geometric features as the periodic bi-material rod in Fig. 1.1 and the following ratio of material properties: $c^{(2)}/c^{(1)} = 2$ and $\rho^{(2)}/\rho^{(1)} = 3$. As in the damped 1D phononic crystal example, we consider a bi-layered unit cell in which $d^{(1)} = d^{(2)}$. In Fig. 1.4, we show these results for a value of wave amplitude of $B = 0.125$. Superimposed, for comparison, are the dispersion curves on the basis of infinitesimal deformation and the corresponding dispersion curves for an equivalent statically homogenized medium (for which the elastic properties are obtained by the standard rule of mixtures). We observe in the figure that the finite-strain dispersion curves asymptotically converge to the infinitesimal and homogenized curves at long wavelengths

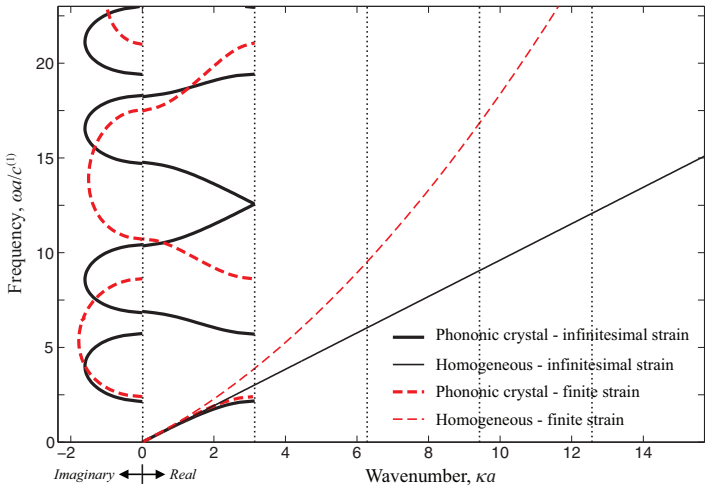

Figure 1.4 Approximate frequency band structure for a 1D phononic crystal under finite deformation [obtained using Eq. (1.53)]. The results shown are for $B = 0.125$. For comparison, the dispersion curves for infinitesimal deformation are included. Also, corresponding dispersion curves for a statically equivalent homogenous rod are overlaid.

as expected. We also note that the finite deformation causes the dispersion branches to rise and the band gaps to increase significantly — an attractive trait for many applications involving sound and vibration control.

References

1. M. Ruzzene, F. Scarpa and F. Soranna, "Wave beaming effects in two-dimensional cellular structures," *Smart Materials and Structures*, **12**, 363–372, 2003.
2. M. I. Hussein, G. M. Hulbert and R. A. Scott, "Dispersive elastodynamics of 1D banded materials and structures: Design," *Journal of Sound and Vibration*, **307**, 865–893, 2007.
3. S. Yang, J. H. Page, Z. Liu, M. L. Cowan, C. T. Chan and P. Sheng, "Focusing of sound in a 3D phononic crystal," *Physical Review Letters*, **93**, 024301, 2004.

4. J. Zhu, J. Christensen, J. Jung, L. Martin-Moreno, X. Yin, L. Fok, X. Zhang and F. J. Garcia-Vidal, "A holey-structured metamaterial for acoustic deep-subwavelength imaging," *Nature Physics*, **7**, 52–55, 2011.
5. S. A. Cummer and D. Schurig, "One path to acoustic cloaking," *New Journal of Physics*, **9**, 45, 2007.
6. D. Torrent and J. Sánchez-Dehesa "Acoustic metamaterials for new two-dimensional sonic devices," *New Journal of Physics*, **9**, 323, 2007.
7. P. E. Hopkins, C. M. Reinke, M. F. Su, R. H. Olsson, E. A. Shaner, Z. C. Leseman, J. R. Serrano, L. M. Phinney and I. El-Kady, "Reduction in the thermal conductivity of single crystalline silicon by phononic crystal patterning," *Nano Letters*, **11**, 107–112, 2011.
8. B. L. Davis and M. I. Hussein, "Thermal characterization of nanoscale-phononic crystals using supercell lattice dynamics," *AIP Advances,* **1**, 041701, 2011.
9. M.-H. Lu, L. Feng and Y.-F. Chen, "Phononic crystals and acoustic metamaterials," *Materials Today*, **12**, 34–42, 2009.
10. N. B. Li, J. Ren, L. Wang, G. Zhang, P. Hänggi and B. W. Li, "*Colloquium*: Phononics: Manipulating heat flow with electronic analogs and beyond," *Review of Modern Physics*, **84**, 1045–1066, 2012.
11. M. I. Hussein and I. El-Kady, "Preface to special topic: Selected articles from Phononics 2011: The First International Conference on Phononic Crystals, Metamaterials and Optomechanics, 29 May-2 June, 201, Santa Fe, New Mexico, USA," *AIP Advances,* **1**, 041301, 2011.
12. M. S. Kushwaha, P. Halevi, L. Dobrzynski and B. Djafari-Rouhani, "Acoustic band-structure of periodic elastic composites," *Physical Review Letters*, **71**, 2022–2025, 1993.
13. M. Sigalas and E. N. Economou, "Band-structure of elastic waves in 2-dimensional systems," *Solid State Communications*, **86**, 141–143, 1993.
14. Z. Y. Liu, X. X. Zhang, Y. W. Mao, Y. Y. Zhu, Z. Y. Yang, C. T. Chan and P. Sheng, "Locally resonant sonic materials," *Science*, **289**, 1734–1736, 2000.
15. F. Bloch, "Über die Quantenmechanik der Electron in Kristallgittern (On the quantum mechanics of electron in crystal lattices)," *Zeifschriftfür Physik*, **52**, 555–600, 1928.
16. C. Croenne, E. J. S. Lee, H. F. Hu and J. H. Page, "Band gaps in phononic crystals: Generation mechanisms and interaction effects," *AIP Advances*, **1**, 041401, 2011.
17. L. Liu and M. I. Hussein, "Wave motion in periodic flexural beams and characterization of the transition between Bragg scattering and local

resonance," *Journal of Applied Mechanics – Transactions of the ASME*, **79**, 011003, 2012.

18. N. Swinteck, S. Bringuier, J.-F. Robillard, J. O. Vasseur, A. C. Hladky-Hennion, K. Runge and P. A. Deymier, "Phase-control in two-dimensional phononic crystals," *Journal of Applied Physics*, **110**, 074507, 2011.
19. J. Christensen, A. I. Fernandez-Dominguez, F. De Leon-Perez, L. Martin-Moreno and F. J. Garcia-Vidal, "Collimation of sound assisted by acoustic surface waves," *Nature Physics*, **3**, 851–852, 2007.
20. O. Sigmund and J. S. Jensen, "Systematic design of phononic band-gap materials and structures by topology optimization," *Philosophical Transactions of the Royal Society of London, series A-Mathematical, Physical and Engineering Sciences*, **361**, 1001–1019, 2003.
21. O. R. Bilal and M. I. Hussein, "Ultrawide phononic band gap for combined in-plane and out-of-plane waves," *Physical Review E*, **84**, 065701(R), 2011.
22. M. I. Hussein, G. M. Hulbert, and R. A. Scott, "Dispersive elastodynamics of 1D banded materials and structures: analysis," *Journal of Sound and Vibration*, **289**, 779–806, 2006.
23. S. Phani, J. Woodhouse and N. A. Fleck, "Wave propagation in two-dimensional periodic lattices," *Journal of the Acoustical Society of America*, **119**, 1995–2005, 2006.
24. S. Nowick and B. S. Berry, Anelastic relaxation in crystalline solids, New York: Academic Press, 1972.
25. W. Bert, "Material damping: An introductory review of mathematic measures and experimental techniques," *Journal of Sound and Vibration*, **29**, 129–153, 1973.
26. J. Woodhouse, "Linear damping models for structural vibration," *Journal of Sound and Vibration*, **215**, 547–569, 1998.
27. M. I. Hussein, "Theory of damped Bloch waves in elastic media," *Physical Review B*, **80**, 212301, 2009.
28. M. I. Hussein and M. J. Frazier, "Band structures of phononic crystals with general damping," *Journal of Applied Physics*, **108**, 093506, 2010.
29. J. W. S. Rayleigh, Theory of sound, London: MaCmillon and Co., 1878.
30. W. G. Cady, "Theory of longitudinal vibrations of viscous rods," *Physical Review*, **19**, 1–6, 1922.
31. S. Mukherjee and E. H. Lee, "Dispersion relations and mode shapes for waves in laminated viscoelastic composites by finite difference methods," *Computers & Structures*, **5**, 279–285, 1975.

32. K. F. Graff, Wave motion in elastic solids, Dover Publications, New York, 1991.
33. J. D. Achenbach, Wave propagation in elastic solids, North-Holland, Amsterdam, 1987.
34. C. Truesdell, "General and exact theory of waves in finite elastic strain," *Archive for Rational Mechanics and Analysis*, **8**, 263–296, 1961.
35. A. E. Green, "A note on wave propagation in initially deformed bodies," *Journal of the Mechanics and Physics of Solids*, **11**, 119–126, 1963.
36. L. K. Zarembo and V. A. Krasilni, "Nonlinear phenomena in the propagation of elastic waves in solids," *Soviet Physics Uspekhi-USSR*, **13**, 778–797, 1971.
37. P. L. Bhatnagar, Nonlinear waves in one-dimensional dispersive systems, Clarendon Press, Oxford, 1979.
38. A. H. Nayfeh, D. T. Mook, Nonlinear oscillations, Wiley-VCH, New York, 1995.
39. R. W. Ogden, Non-linear elastic deformations, Dover Publications, New York, 1997.
40. A. N. Norris, Finite amplitude waves in solids, In: M. F. Hamilton and D. T. Blackstock (Eds.), Nonlinear Acoustics, 263–277, Academic Press, San Diego, 1999.
41. M. Destrade and G. Saccomandi, "Introduction to the special issue on waves in non-linear solid mechanics," *International Journal of Non-linear Mechanics*, **44**, 445–449, 2009.
42. S. W. Shaw and C. Pierre, "Normal modes for nonlinear vibratory systems," *Journal of Sound and Vibration*," **164**, 85–124, 1993.
43. P. Gumbsch and H. Gao, "Dislocations faster than the speed of sound," *Science*, **283**, 965–968, 1999.
44. A. J. Rosakis, O. Samudrala and D. Coker, "Cracks faster than the shear wave speed," *Science*, **284**, 1337–1340, 1999.
45. L. A. Ostrovsky and P. A. Johnson, "Dynamic nonlinear elasticity in geomaterials," *Rivista Del Nuovo Cimento*, **24**, 1–46, 2001.
46. Y. Zheng, R. G. Maev and I. Y. Solodov, "Nonlinear acoustic applications for material characterization: A review," *Canadian Journal of Physics*, **77**, 927–967, 1999.
47. K. E. A. Van Den Abeele, P. A. Johnson and A. Sutin, "Nonlinear elastic wave spectroscopy techniques to discern material damage, part I: Non-linear wave modulation spectroscopy," *Research in Nondestructive Evaluation*, **12**, 17–30, 2000.

48. B. Ward, A. C. Baker and V. F. Humphrey, "Nonlinear propagation applied to the improvement of resolution in diagnostic medical ultrasound," *Journal of the Acoustical Society of America*, **101**, 143–154, 1997.
49. P. Boulanger and M. Hayes, "Finite-amplitude waves in deformed Mooney-Rivlin materials," *Quarterly Journal of Mechanics and Applied Mathematics*, **45**, 575–593, 1992.
50. P. Boulanger, M. Hayes and C. Trimarco, "Finite-amplitude plane waves in deformed Hadamard elastic materials," *Geophysical Journal International*, **118**, 447–458, 1994.
51. M. Destrade and G. Saccomandi, "Nonlinear transverse waves in deformed dispersive solids," *Wave Motion*, **45**, 325–336, 2008.
52. T. Wright, "Nonlinear-waves in rods: results for incompressible elastic-materials," *Studies in Applied Mathematics*, **72**, 149–160, 1985.
53. B. D. Coleman and D. C. Newman, "On waves in slender elastic rods," *Archive for Rational Mechanics and Analysis*, **109**, 39–61, 1990.
54. A. M. Samsonov, Nonlinear strain waves in elastic waveguides, In: A. Jeffrey, J. Engelbreght (Eds.), Nonlinear Waves in Solids, 349–382, Springer, New York, 1994.
55. H. H. Dai, "Model equations for nonlinear dispersive waves in a compressible Mooney-Rivlin rod," *ActaMechanica*, **127**, 193–207, 1998.
56. H. H. Dai and Y. Huo, "Solitary shock waves and other travelling waves in a general compressible hyperelastic rod," *Proceedings of the Royal Society of London Series A – Mathematical, Physical and Engineering Sciences*, **456**, 331–363, 2000.
57. S. Y. Zhang and Z. F. Liu, "Three kinds of nonlinear dispersive waves in elastic rods with finite deformation," *Applied Mathematics and Mechanics (English Edition)*, **29**, 909–917, 2008.
58. A. F. Vakakis and M. E. King, "Nonlinear wave transmission in a monocoupled elastic periodic system," *Journal of the Acoustical Society of America*, **98**, 1534–1546, 1995.
59. K. Manktelow, M. J. Leamy, and M. Ruzzene, "Multiple scales analysis of wave-wave interactions in a cubically nonlinear monoatomic chain," *Nonlinear Dynamics*, **63**, pp. 193–203, 2011.
60. G. Chakraborty and A. K. Mallik, "Dynamics of a weakly non-linear periodic chain," *International Journal of Non-linear Mechanics*, **36**, 375–389, 2001.
61. R. K. Narisetti, M. J. Leamy and M. Ruzzene, "A perturbation approach for predicting wave propagation in one-dimensional nonlinear periodic structures," *Journal of Vibration and Acoustics*, **132**, 031001, 2010.

62. B. S. Lazarov and J. S. Jensen, "Low-frequency band gaps in chains with attached non-linear oscillators," *International Journal of Non-Linear Mechanics*, **42**, 1186–1193, 2007.
63. R. K. Narisetti, M. Ruzzene and M. J. Leamy, "Study of wave propagation in strongly nonlinear periodic lattices using a harmonic balance approach," *Wave Motion*, **49**, 394–410, 2012.
64. E. Herbold, J. Kim, V. Nesterenko, S. Wang and C. Daraio, "Pulse propagation in a linear and nonlinear diatomic periodic chain: effects of acoustic frequency band-gap," *Acta Mechanica*, **205**, 85–103, 2009.
65. M. H. Abedinnasab and M. I. Hussein, "Wave dispersion under finite deformation," *Wave Motion*, 2012, doi:10.1016/j.wavemoti.2012.10.008.
66. J. Billingham, A. C. King, Wave motion, Cambridge University Press, Cambridge, 2000.
67. The MathWorks Inc., 2009. URL: http://www.mathworks.com.